Secure Control Regions for Distributed Stochastic Systems with Application to Distributed Energy Resource Dispatch

Preprint

Joshua Comden, Ahmed S. Zamzam, and Andrey Bernstein

National Renewable Energy Laboratory

Presented at the 2022 American Control Conference (ACC)
Atlanta, Georgia
June 8-10, 2022

NREL is a national laboratory of the U.S. Department of Energy
Office of Energy Efficiency & Renewable Energy
Operated by the Alliance for Sustainable Energy, LLC

This report is available at no cost from the National Renewable Energy Laboratory (NREL) at www.nrel.gov/publications.

Contract No. DE-AC36-08GO28308

Conference Paper
NREL/CP-5D00-81300
June 2022

Secure Control Regions for Distributed Stochastic Systems with Application to Distributed Energy Resource Dispatch

Preprint

Joshua Comden, Ahmed S. Zamzam, and Andrey Bernstein

National Renewable Energy Laboratory

Suggested Citation
Comden, Joshua, Ahmed S. Zamzam, and Andrey Bernstein. 2022. *Secure Control Regions for Distributed Stochastic Systems with Application to Distributed Energy Resource Dispatch: Preprint*. Golden, CO: National Renewable Energy Laboratory. NREL/CP-5D00-81300. https://www.nrel.gov/docs/fy22osti/81300.pdf.

Conference Paper
NREL/CP-5D00-81300
June 2022

National Renewable Energy Laboratory
15013 Denver West Parkway
Golden, CO 80401
303-275-3000 • www.nrel.gov

NOTICE

This work was authored by the National Renewable Energy Laboratory, operated by Alliance for Sustainable Energy, LLC, for the U.S. Department of Energy (DOE) under Contract No. DE-AC36-08GO28308. Funding provided by the U.S. Department of Energy Office of Energy Efficiency and Renewable Energy Solar Energy Technologies Office. The views expressed herein do not necessarily represent the views of the DOE or the U.S. Government. The U.S. Government retains and the publisher, by accepting the article for publication, acknowledges that the U.S. Government retains a nonexclusive, paid-up, irrevocable, worldwide license to publish or reproduce the published form of this work, or allow others to do so, for U.S. Government purposes.

Cover Photos by Dennis Schroeder: (clockwise, left to right) NREL 51934, NREL 45897, NREL 42160, NREL 45891, NREL 48097, NREL 46526.

Secure Control Regions for Distributed Stochastic Systems with Application to Distributed Energy Resource Dispatch

Joshua Comden, Ahmed S. Zamzam, and Andrey Bernstein

***Abstract*— With the increasing connectedness and interdependence of systems that are stochastic in nature, the issue of how to manage and coordinate them for safe operation has evidently become more important. In many networked system architectures, the system-wide output must be delicately managed, often within a prescribed set of bounds. In this paper, a novel control framework is proposed where the bounds on the outputs are translated into *independent* bounds on the controllable inputs of each subsystem. The main benefit of this framework is that respecting the individual control bounds suffices to guarantee that the system-wide outputs will remain within safe boundaries. Because the systems are assumed to be stochastic, the bounds on the output are introduced as probabilistic chance constraints. The benefits of this framework are demonstrated by applying it to the control of distributed energy resources in a distribution network where the main goal is to keep the voltage magnitudes within their prescribed bounds. The control bounds are evaluated using real data on an IEEE test system.**

I. Introduction

This paper considers the problem of controlling a networked stochastic system so that each of its outputs is probabilistically guaranteed to be within a given set of bounds. More specifically, we consider the following stochastic model:

$$\mathbf{y} = \mathbf{A}\mathbf{x} + \mathbf{b} \tag{1}$$

where $\mathbf{x} \in \mathbb{R}^n$ is the vector of the controllable system inputs, $\mathbf{y} \in \mathbb{R}^m$ is the vector of the system outputs, and $[\mathbf{A} \quad \mathbf{b}] \in \mathbb{R}^{m\times(n+1)}$ is a matrix of random variables. The goal is to control the system inputs, $\mathbf{x}$, so that the system outputs, $\mathbf{y}$, stay between the given bounds, $\underline{\mathbf{y}} \in \mathbb{R}^m$ and $\overline{\mathbf{y}} \in \mathbb{R}^m$, under the following probabilistic conditions:

$$\Pr\big(\underline{y}_j \le y_j\big) \ge 1 - \underline{\alpha}_j, \quad \forall j \in \{1,\dots,m\} \tag{2a}$$

$$\Pr\big(y_j \le \overline{y}_j\big) \ge 1 - \overline{\alpha}_j, \quad \forall j \in \{1,\dots,m\} \tag{2b}$$

where $\underline{\alpha}_j \in (0,1) : \forall j \in \{1,\dots,m\}$ and $\overline{\alpha}_j \in (0,1) : \forall j \in \{1,\dots,m\}$ are the elementwise allowable probabilities of violation for the lower and upper bounds, respectively.

The authors are with the Power Systems Engineering Center at the National Renewable Energy Laboratory, Golden, CO, USA.

This work was authored by the National Renewable Energy Laboratory, operated by Alliance for Sustainable Energy, LLC, for the U.S. Department of Energy (DOE) under Contract No. DE-AC36-08GO28308. Funding provided by the U.S. Department of Energy Office of Energy Efficiency and Renewable Energy Solar Energy Technologies Office Award Number DE-EE0009023. The views expressed in the article do not necessarily represent the views of the DOE or the U.S. Government. The U.S. Government retains and the publisher, by accepting the article for publication, acknowledges that the U.S. Government retains a nonexclusive, paid-up, irrevocable, worldwide license to publish or reproduce the published form of this work, or allow others to do so, for U.S. Government purposes.

Many stochastic control schemes involve measuring and reacting globally to near-instantaneous realizations of the random variables. For some networked stochastic systems, however, this could require expensive, ultrareliable, low-latency communication equipment, whereas low-cost slower communication equipment might already be in place or more feasible to implement. Our approach will be to design a control scheme for the latter equipment scenario of not being able to near-instantaneously measure and react globally. Specifically, our goal is to find bounds, $\{\underline{\mathbf{x}}, \overline{\mathbf{x}}\} \in \mathbb{R}^n$, on the controllable inputs, $\mathbf{x}$, so that the conditions given in (2) are satisfied for any $\mathbf{x}$ between their elementwise lower, $\underline{\mathbf{x}}$, and upper, $\overline{\mathbf{x}}$, bounds.

The main benefit of this decision structure is that after the bounds $(\underline{\mathbf{x}}, \overline{\mathbf{x}})$ are calculated, each element of the input, $\mathbf{x}$, can be optimized or controlled independently without communication for some other objective, especially a local objective. In fact, if the bounds $(\underline{\mathbf{x}}, \overline{\mathbf{x}})$ are set for long time intervals, a future set of bounds could be decided upon while another is in place, making the system resistant to the effects of communication failures.

In the robust optimization community, there is a special class of problems called grey or interval optimization that treats all decision variables and system parameters as intervals that can take any value between their lower and upper bounds [1]. The system parameter intervals are meant to capture uncertainty in the system, and the decision variable intervals are meant to represent ranges of decisions that would result in bounded costs. This method has been applied to waste management [2], hydropower scheduling [3], economic dispatch [4], and heat transfer problems [5].

Also, similar to the objective of the framework described in our paper, there is other work on decomposing optimization problems into different timescales. For example, the work by [6], [7] splits an optimal control problem into fast-acting decentralized controllers and a slow, centralized controller that coordinates the decentralized ones. The benefit of our framework is that we do not impose any special structure of the fast controller other than respecting the control bounds.

In this paper, we make the following contributions:

- We formulate a novel general chance-constrained control bound problem of a networked stochastic system (Section II).
- We reformulate the infinite set of chance constraints stated in the general control bound problem to a finite set (Section III).
- We apply the general control bound problem to the

control of distributed energy resources (DERs) in a distribution network to keep the voltage magnitudes within a given range (Section IV).
- We calculate and evaluate the control bounds of DERs with real-world data and show that the control bounds are able to respect the chance constraints used to bound the voltage magnitudes across a distribution network (Section V).

II. Problem Formulation

Consider a system comprising of K subsystems. Let the input of each subsystem, k, be denoted by $\mathbf{x}_k \in \mathbb{R}^{n_k}$, then define $\mathbf{x} := \begin{bmatrix}\mathbf{x}_1^\top & \dots & \mathbf{x}_K^\top\end{bmatrix}^\top \in \mathbb{R}^n$, i.e., we have $\sum_{k=1}^K n_k = n$. Likewise, we partition and label the bounds on the controllable inputs $(\underline{\mathbf{x}}, \overline{\mathbf{x}})$ so that the bounds on the input of the k-th subsystem are denoted by $(\underline{\mathbf{x}}_k, \overline{\mathbf{x}}_k)$. Consider the following stochastic optimization problem to decide the independent control bounds for each subsystem:

$$\max_{\underline{\mathbf{x}},\overline{\mathbf{x}}} \quad \sum_{k=1}^{K} \omega_k f_k(\underline{\mathbf{x}}_k, \overline{\mathbf{x}}_k) \tag{3a}$$

$$\text{s.t.} \quad \Pr\big(\underline{y}_j \le \mathbf{A}_j\mathbf{x} + b_j\big) \ge 1 - \underline{\alpha}_j, \quad \forall \mathbf{x} \in [\underline{\mathbf{x}}, \overline{\mathbf{x}}], \forall j \in \{1,\dots,m\} \tag{3b}$$

$$\Pr\big(\mathbf{A}_j\mathbf{x} + b_j \le \overline{y}_j\big) \ge 1 - \overline{\alpha}_j, \quad \forall \mathbf{x} \in [\underline{\mathbf{x}}, \overline{\mathbf{x}}], \forall j \in \{1,\dots,m\} \tag{3c}$$

$$\underline{\mathbf{x}} \le \overline{\mathbf{x}} \tag{3d}$$

where $\mathbf{A}_j$ denotes the j-th row of the matrix $\mathbf{A}$, and $\begin{bmatrix}\mathbf{A}_j & b_j\end{bmatrix}^\top \in \mathbb{R}^{(n+1)}$ is a vector of random variables.

The functions $f_k : \forall k \in \{1,\dots,K\}$ are used to characterize a measure of the flexibility in each input that the optimization problem seeks to maximize. In addition, the weights, ω_k, determine how much flexibility each subsystem gets. A common choice of f_k is $f_k(\underline{\mathbf{x}}_k, \overline{\mathbf{x}}_k) = \sum_{j=1}^{n_k} \ln(\overline{x}_{k,j} - \underline{x}_{k,j})$, which implies that (3a) maximizes the volume of the hyperrectangle $(\overline{\mathbf{x}}_k - \underline{\mathbf{x}}_k)$. Also, if there is an operating point, $\mathbf{x}_{k,\text{op}}$, that is desired to be within the bounds, then setting $f_k(\underline{\mathbf{x}}_k, \overline{\mathbf{x}}_k) = -\sum_{j=1}^{n_k}(\max\{0, \underline{x}_{k,j} - x_{k,\text{op},j}\} + \max\{0, x_{k,\text{op},j} - \overline{x}_{k,j}\})$ will promote the bounds $(\underline{\mathbf{x}}, \overline{\mathbf{x}})$ to surround $\mathbf{x}_{\text{op}}$.

After solving Problem (3) for the control bounds $(\underline{\mathbf{x}}, \overline{\mathbf{x}})$, each subsystem, k, will then independently be able to operate its controllable inputs, $\mathbf{x}_k$, anywhere between $\underline{\mathbf{x}}_k$ and $\overline{\mathbf{x}}_k$ while satisfying the global chance constraints (2). Moreover, if the control bounds are intended to be used for multiple instances of time, then each subsystem can move $\mathbf{x}_k$ between the control bounds over time as conditions and objectives change.

III. Chance Constraint Reformulation

The chance constraints in Problem (3) represent an infinite set of constraints because they must hold for every $\mathbf{x}$ between the control bounds $(\underline{\mathbf{x}}, \overline{\mathbf{x}})$. This presents a significant obstacle to implementing these constraints. The following proposition reduces the infinite set to a single chance constraint for each j.

Proposition 1. *Let $\mathbf{a} \in \mathbb{R}^n$ be a vector of random variables. The following set of infinite set of chance constraints:*

$$Pr\left(\mathbf{a}^\top\mathbf{x} \le 0\right) \ge 1 - \alpha, \quad \forall \mathbf{x} \in [\underline{\mathbf{x}}, \overline{\mathbf{x}}] \tag{4}$$

is equivalent to the following chance constraint:

$$Pr\left(\left(\mathbf{a}^-\right)^\top \underline{\mathbf{x}} + \left(\mathbf{a}^+\right)^\top \overline{\mathbf{x}} \le 0\right) \ge 1 - \alpha \tag{5}$$

where $a_i^- := \min\{0, a_i\}$ and $a_i^+ := \max\{0, a_i\}$ separate out the negative and positive elements of $\mathbf{a}$ into two vectors of their negative and positive realizations.

Proof. The infinite set of chance constraints described by Equation (4) are satisfied if and only if the worst-case chance constraint among them is satisfied:

$$\min_{\mathbf{x}\in[\underline{\mathbf{x}},\overline{\mathbf{x}}]} \left\{\Pr\left(\mathbf{a}^\top\mathbf{x} \le 0\right)\right\} \ge 1 - \alpha.$$

which occurs when the LHS of the inequality inside the probability operator is maximized:

$$\min_{\mathbf{x}\in[\underline{\mathbf{x}},\overline{\mathbf{x}}]} \left\{\Pr\left(\mathbf{a}^\top\mathbf{x} \le 0\right)\right\} = \Pr\left(\max_{\mathbf{x}\in[\underline{\mathbf{x}},\overline{\mathbf{x}}]} \left\{\mathbf{a}^\top\mathbf{x}\right\} \le 0\right).$$

Also, we have that:

$$\begin{aligned}\max_{\mathbf{x}\in[\underline{\mathbf{x}},\overline{\mathbf{x}}]} \left\{\mathbf{a}^\top\mathbf{x}\right\} &= \sum_{i=1}^{n} \max_{x_i\in[\underline{x}_i,\overline{x}_i]} a_i x_i \\ &= \left(\mathbf{a}^-\right)^\top \underline{\mathbf{x}} + \left(\mathbf{a}^+\right)^\top \overline{\mathbf{x}}\end{aligned}$$

because the optimization problem is element-wise separable where each element is maximized at either the lower or upper bound of the interval depending on whether a_i is negative or positive. Putting this final expression into the chance constraint gives us the resultant. □

Applying Proposition 1 to the infinite sets of chance chance constraints (3b) and (3c) turns them into the following finite set:

$$\Pr\big(\underline{y}_j \le \mathbf{A}_j^-\overline{\mathbf{x}} + \mathbf{A}_j^+\underline{\mathbf{x}} + b_j\big) \ge 1 - \underline{\alpha}_j, \ \forall j \in \{1,\dots,m\} \tag{6a}$$

$$\Pr\big(\mathbf{A}_j^-\underline{\mathbf{x}} + \mathbf{A}_j^+\overline{\mathbf{x}} + b_j \le \overline{y}_j\big) \ge 1 - \overline{\alpha}_j, \ \forall j \in \{1,\dots,m\}. \tag{6b}$$

IV. Application to Distributed Energy Resource Control

In this section, we apply the general formulation (3) to the control of DERs in a power distribution network. The increased deployment of DERs in a distribution network has made it challenging to control certain state variables of the network. The typical example is voltage regulation, wherein the goal is to operate DERs such that the nodal voltage magnitudes lie within safe bounds. The main challenge is that certain DERs, such as solar panels and wind turbines, add more volatility and uncertainty to the nodal power demand. Moreover, storage devices (e.g., batteries and thermal storage loads) add extra control capabilities that increase the number of dimensions and the complexity of the control decision space.

Communication-based approaches for real-time DER control might be impractical because the communication network that is typically deployed between smart meters and the utility does not allow for continuous bidirectional streaming of measurement data and control signals [8], [9]. Instead, smart meters are often able to send their measurement data in large batches at different time instances; thus, we adopt the general temporal decomposition framework, where the utility sends control signals and collects measurement data at a slow timescale to and from faster-acting DERs [10].

The main task in voltage regulation is to keep the voltage magnitude at each bus in a distribution network between a set of operational bounds. Consider a distribution network with N buses labeled $\{1,\dots,N\}$ and a slack bus labeled 0. The active and reactive power injections for all the (non-slack) buses are denoted by $\mathbf{p}\in\mathbb{R}^N$ and $\mathbf{q}\in\mathbb{R}^N$, respectively. The voltage magnitudes, denoted by $\mathbf{v}\in\mathbb{R}^N$, can be approximately represented by the following equation:

$$\mathbf{v}=\mathbf{R}\mathbf{p}+\mathbf{B}\mathbf{q}+\mathbf{a} \tag{7}$$

where $\mathbf{R}\in\mathbb{R}^{N\times N}$, $\mathbf{B}\in\mathbb{R}^{N\times N}$, and $\mathbf{a}\in\mathbb{R}^N$ are matrices of system parameters. Equation (7) is a linearization of nonlinear power flow equations that we assume is stochastic in nature. For example, the linearization method developed by [11] uses the nodal admittance matrix to calculate the parameters $(\mathbf{R},\mathbf{B},\mathbf{a})$; however, there can be uncertainty in calculating the admittance matrix because of uncertainties in the resistance values of the distribution lines that are partially caused by their dependence on temperature [12]. Thus, the randomness in the resistance values of the lines results in random system parameters $(\mathbf{R},\mathbf{B},\mathbf{a})$.

We partition the power injections $(\mathbf{p},\mathbf{q})$ into controllable parts $(\mathbf{p}^{\text{ctr}},\mathbf{q}^{\text{ctr}})$ comprising the controllable DERs and uncontrollable parts $(\mathbf{p}^{\text{unc}},\mathbf{q}^{\text{unc}})$ comprising uncontrollable DERs and loads so that:

$$\mathbf{p}=\mathbf{p}^{\text{ctr}}+\mathbf{p}^{\text{unc}} \tag{8a}$$

$$\mathbf{q}=\mathbf{q}^{\text{ctr}}+\mathbf{q}^{\text{unc}} \tag{8b}$$

where we model $(\mathbf{p}^{\text{unc}},\mathbf{q}^{\text{unc}})$ as vectors of random variables, and we specify that the bus-wise controllable variables must fit within a local control space, $\mathcal{X}_i$, specifically $(p_i^{\text{ctr}},q_i^{\text{ctr}})\in\mathcal{X}_i:\forall i\in\{1\dots,N\}$.

Based on the control bound framework described in Section II, our goal is to find the lower $(\underline{\mathbf{p}}^{\text{ctr}},\underline{\mathbf{q}}^{\text{ctr}})$ and upper $(\overline{\mathbf{p}}^{\text{ctr}},\overline{\mathbf{q}}^{\text{ctr}})$ control bounds so that the voltage magnitudes, $\mathbf{v}$, at each bus stay within the lower $\underline{\mathbf{v}}$ and upper $\overline{\mathbf{v}}$ bounds with a probability of at least $1-\alpha$ for any choice of control variable $(\mathbf{p}^{\text{ctr}},\mathbf{q}^{\text{ctr}})$ between the bounds. More specifically, with the use of quations (7) and (8), we want to satisfy the following infinite set of chance constraints:

$$\Pr\big(\underline{v}_i\le v_i\big)\ge 1-\frac{\alpha}{2},\forall\mathbf{p}^{\text{ctr}}\in\left[\underline{\mathbf{p}}^{\text{ctr}},\overline{\mathbf{p}}^{\text{ctr}}\right],\forall\mathbf{q}^{\text{ctr}}\in\left[\underline{\mathbf{q}}^{\text{ctr}},\overline{\mathbf{q}}^{\text{ctr}}\right],\quad\forall i\in\{1,\dots,N\} \tag{9a}$$

$$\Pr\big(v_i\le\overline{v}_i\big)\ge 1-\frac{\alpha}{2},\forall\mathbf{p}^{\text{ctr}}\in\left[\underline{\mathbf{p}}^{\text{ctr}},\overline{\mathbf{p}}^{\text{ctr}}\right],\forall\mathbf{q}^{\text{ctr}}\in\left[\underline{\mathbf{q}}^{\text{ctr}},\overline{\mathbf{q}}^{\text{ctr}}\right],\quad\forall i\in\{1,\dots,N\} \tag{9b}$$

where the probability of violation, $\alpha\in(0,1)$, is split equally between the upper and lower voltage magnitude bounds. Using the chance constraint reformulation in Equation (6), the aforementioned chance constraints become:

$$\Pr\big(\underline{v}_i\le\mathbf{R}_i^-\overline{\mathbf{p}}^{\text{ctr}}+\mathbf{B}_i^-\overline{\mathbf{q}}^{\text{ctr}}+\mathbf{R}_i^+\underline{\mathbf{p}}^{\text{ctr}}+\mathbf{B}_i^+\underline{\mathbf{q}}^{\text{ctr}}+w_i\big)\ge 1-\frac{\alpha}{2},\quad\forall i\in\{1,\dots,N\} \tag{10a}$$

$$\Pr\big(\mathbf{R}_i^-\underline{\mathbf{p}}^{\text{ctr}}+\mathbf{B}_i^-\underline{\mathbf{q}}^{\text{ctr}}+\mathbf{R}_i^+\overline{\mathbf{p}}^{\text{ctr}}+\mathbf{B}_i^+\overline{\mathbf{q}}^{\text{ctr}}+w_i\le\overline{v}_i\big)\ge 1-\frac{\alpha}{2},\quad\forall i\in\{1,\dots,N\} \tag{10b}$$

where $\mathbf{w}:=\mathbf{R}\mathbf{p}^{\text{unc}}+\mathbf{B}\mathbf{q}^{\text{unc}}+\mathbf{a}$ is a vector of the random variables containing the randomness from the uncontrollable loads and the uncertain system parameters.

The randomness observed by the uncontrollable loads $(\mathbf{p}^{\text{unc}},\mathbf{q}^{\text{unc}})$ can be defined at a finer temporal granularity than that of the control bounds $(\underline{\mathbf{p}}^{\text{ctr}},\underline{\mathbf{q}}^{\text{ctr}},\overline{\mathbf{p}}^{\text{ctr}},\overline{\mathbf{q}}^{\text{ctr}})$. For example, if the control bounds are defined for a 15-min interval, the randomness in the uncontrollable loads can be defined for the 1-min intervals within it. Also, it means that the controllable DERs could modulate $(\mathbf{p}^{\text{ctr}},\mathbf{q}^{\text{ctr}})$ in response to the observed local uncontrollable loads or objectives that change faster than every 15 minutes as long as they remain within their control bounds.

Note that this single-period problem for determining DER control bounds can be extended to the multiperiod problem if the necessary information is available. For example, the control bounds could be defined in a day-ahead framework if, for every time interval in a day, there is an associated multivariate probability distribution that describes the uncontrollable power injections $(\mathbf{p}^{\text{unc}},\mathbf{q}^{\text{unc}})$ and the system parameters $(\mathbf{R},\mathbf{B},\mathbf{a})$, and there are sets, $\mathcal{X}_i:\forall i\in\{1,\dots,N\}$, that bound the controllable power injections $(\mathbf{p}^{\text{ctr}},\mathbf{q}^{\text{ctr}})$. Note that in this case, the set $\mathcal{X}_i$ is coupled in time (e.g., for thermal loads and batteries), but the methods described by, e.g., [13], [14], can handle this by computing a conservative inner approximation of their Cartesian product. Consequently, the obtained control bounds will be more conservative for larger control horizons.

V. Distributed Energy Resource Control Numerical Simulations

In this section, we demonstrate the efficacy of the lower bounds $(\underline{\mathbf{p}}^{\text{ctr}},\underline{\mathbf{q}}^{\text{ctr}})$ and upper bounds $(\overline{\mathbf{p}}^{\text{ctr}},\overline{\mathbf{q}}^{\text{ctr}})$ on the controllable power injections, which are computed using the proposed method for a distribution network under a realistic scenario.

A. Setup

Suppose that a system operator (utility) sends out a day-ahead sequence of time-varying control bounds, $\{\underline{p}_i^{\text{ctr}}(t),\underline{q}_i^{\text{ctr}}(t),\overline{p}_i^{\text{ctr}}(t),\overline{q}_i^{\text{ctr}}(t)\}:\forall t\in\mathcal{T}$, to each bus $i\in\{1,\dots,N\}$, where $\mathcal{T}$ contains all the time intervals of a day. The controllable DERs located at each bus can operate according to their individual objectives as long as their net power injection remains within the control bounds. Because the utility sets the control bounds to satisfy the chance

constraints stated in Equation (10), the day-ahead voltage profile at each bus, i, is guaranteed to remain within its bounds $(\underline{v}_i, \overline{v}_i)$, with a probability of at least $1-\alpha$. We assume that the utility receives the time-varying, day-ahead control space, $\mathcal{X}_i(t) : \forall t \in \mathcal{T}$, from each bus, i.

The time-series data used in the numerical simulations were derived from the Pecan Street Dataport [15] and processed by a research team at the Eaton Corporation for a set of homes from Austin, Texas, at 1-min granularity, split among the devices used in the homes. The devices were partitioned into controllable devices (heating, ventilating, and air conditioning; battery; curtailable photovoltaics (PV)) and all other uncontrollable devices. For each home, the feasible control space was found by using a temperature comfort range within the home and simulating the time-varying minimum and maximum possible load that keeps the home within the temperature range. The uncontrollable devices from all the homes were aggregated together and forecasted in a day-ahead manner. This was done for the 31 days prior to the day being analyzed in this section to get the historical data of the forecasting errors. There were 2 days being analyzed: August 17, 2020, with 14 homes, and December 8, 2020, with 18 homes.

We use the bootstrapping statistical method to generate a synthetic data set from the processed home data in the following manner. For spatial diversity of the feasible control space during a particular day at each bus in the distribution network, we randomly select homes with replacement and sum together the upper and lower bounds, respectively, of their feasible control spaces to form $\mathcal{X}_i(t) : \forall t \in \mathcal{T}$. The number of homes selected is equal to the number of homes available for that day so that the values are scaled appropriately with the aggregated uncontrollable devices from the same number of homes. For temporal and historical diversity of the uncontrollable loads at each bus, we randomly select days with replacement and concatenate their associated forecasts and realizations of the aggregated uncontrollable devices together. This gives a similar but diverse history for each bus, which can be then used to find the means and covariance matrix across the buses of the forecasting errors.

The power system used in the numerical simulations is the IEEE 33-bus distribution network [16]. The loads from the previously described data are scaled so that their mean aligns with the default settings of the test case. To add uncertainty and randomness in the power system model, we randomly distribute the resistances of all the lines in a uniform distribution, $\pm 20\%$ from their nominal values, as described by [12]. For each sampled network-wide realization of resistances, the resulting impedances are converted into a nodal admittance matrix. Using the linearization method from [11], we convert the admittance matrix into the system parameters $(\mathbf{R}, \mathbf{B}, \mathbf{a})$; thus, from every network-wide realization of resistances, we have a separate realization of the system parameters $(\mathbf{R}, \mathbf{B}, \mathbf{a})$, which is used to build an empirical distribution from 1000 samples and find the mean and covariances between the elements. For this simulation, we separately linearize around $\underline{\mathbf{v}}$ and $\overline{\mathbf{v}}$ to get two sets of system parameters $(\mathbf{R}, \mathbf{B}, \mathbf{a})$: one for the chance constraints on the lower bounds and one for the chance constraints on the upper bounds. Although the probability distributions are based on the linearized power flows, the resulting voltages used in the evaluation of the control bounds are simulated using the nonlinear ac power flow equations in PandaPower [17].

To find the control bounds, we solve the following optimization problem for each time, $t \in \mathcal{T}$, at 15-min granularity:

$$\max_{\underline{\mathbf{p}}^{\text{ctr}}, \overline{\mathbf{p}}^{\text{ctr}}, \underline{\mathbf{q}}^{\text{ctr}}, \overline{\mathbf{q}}^{\text{ctr}}} \quad \sum_{i=1}^{N} \ln(\overline{p}_i^{\text{ctr}} - \underline{p}_i^{\text{ctr}}) + \sum_{i=1}^{N} \ln(\overline{q}_i^{\text{ctr}} - \underline{q}_i^{\text{ctr}}) \quad \text{(11a)}$$

$$\text{s.t.} \quad (10) \quad \text{(11b)}$$

$$\{(\underline{p}_i^{\text{ctr}}, \underline{q}_i^{\text{ctr}}), (\overline{p}_i^{\text{ctr}}, \overline{q}_i^{\text{ctr}})\} \in \mathcal{X}_i(t), \quad \forall i \in \{1 \dots, N\} \quad \text{(11c)}$$

where the goal is to spread out the control flexibility widely among the buses, the probability of violation α was set to 0.1, and the voltage bounds were set to 0.95 and 1.05 p.u. at each bus. Because the chance constraints stated in (10) cannot be directly coded into a solver, we use the sample mean and covariance matrix to form the distributionally robust convex equivalents for which we assume the sample mean and covariance are approximately the true versions (See [18], Section 3.1). Note that the work by [19] can deal with the uncertainty that comes from using the sample mean and covariance in place of their unknown true versions. As a benchmark, we compare the use of control bounds to not having bounds on control, i.e., each bus can operate anywhere in their feasible space, $\mathcal{X}_i(t)$, at any time t.

B. Results

Because of space limitations, we focus on simulations based on the data from August 17, 2020, and we showcase Bus 26 as indexed by [16] because it displays many features found on the other buses. Figure 1 displays the normalized control bound sizes of each bus during the day that are calculated as the difference between the upper and lower control bounds. Depending on its location in the network, a bus has more or less control flexibility, especially between the hours of 10 through 18, when there is a significant amount of available generation from solar. The simulations based on data from December 8, 2020, show similar characteristics but have less dynamic profiles.

A sample of the lower and upper control bounds are shown in Figure 2 for both their active and reaction parts. For the first 10 hours and last 4 hours of the day, the control bounds have no restrictions and are equivalent to the feasible bounds set by the control capabilities at the bus. At hours 10 through 16, the control bounds expand but are limited relative to the potential expansion because every other bus in the network can also expand from the available PV power; the natural log in Problem (11) spreads the potential control space among the buses.

Because there are infinite choices for each bus within its control or feasible bounds, we simulate two extreme scenarios for both the case when control bounds are implemented

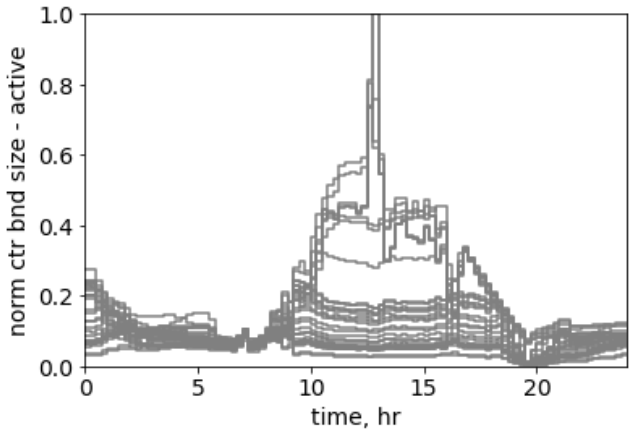

(a) Active load

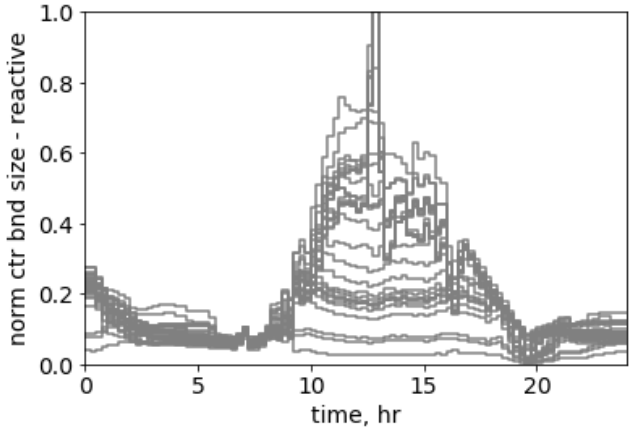

(b) Reactive load

Fig. 1: Control bound sizes of each bus vs. time, normalized by their maximum feasible space size.

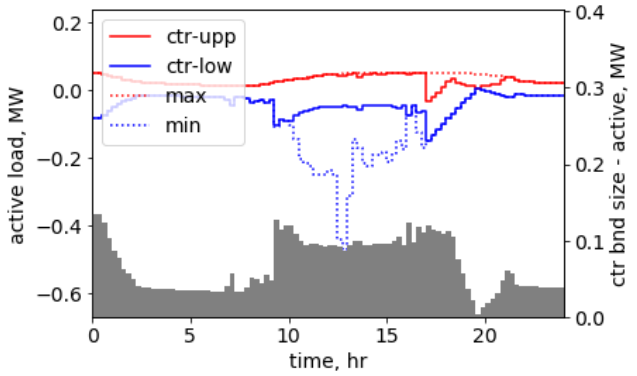

(a) Active load

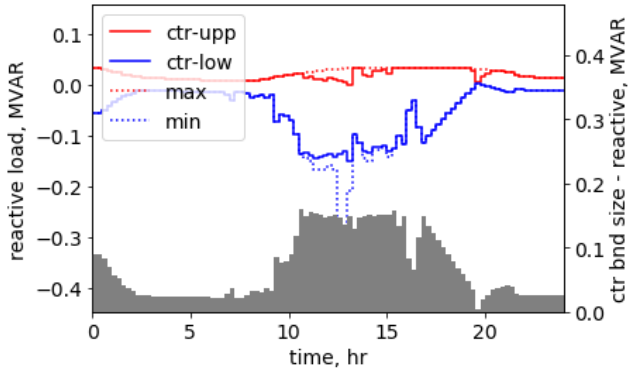

(b) Reactive load

Fig. 2: Upper and lower control bounds vs. time of Bus 26 compared to their maximum and minimum feasible bounds. The gray bars along the bottom of each plot show the distance between the upper and lower control bounds.

versus when they are not: (i) all controllable power injections go to their minimum possible values, and (ii) all controllable power injections go to their maximum possible values. These two extreme scenarios under control bounds will push the chance constraints (9) to their limits, and under no control bounds, they will show the potential consequences without them.

Figure 3a shows these extreme scenarios for a single day, which includes the realized forecasting errors of the uncontrollable loads and the random realizations of the line resistances. Under the case with control bounds, the voltage magnitudes stay within or very close to their limits of (0.95, 1.05) p.u., whereas the case without control bounds goes below 0.90 p.u. and above 1.40 p.u. Observe that right before hour 20, the feasible control spaces pushes the maximum possible voltage magnitude down to almost its lower limit of 0.95 p.u., whereas the upper control bound holds the voltage magnitude to be above 0.95 p.u. This is also shown in Figure 2 where the control bounds almost collapse to a single point.

To evaluate the satisfaction of the chance constraints (9), Figure 3b gives two histograms when the controllable loads are all at their upper bounds (left) and all at their lower bounds (right). The forecasting errors from all 32 days and the random realizations of the line resistances were used to generate the histograms. The red triangles locate the $\frac{\alpha}{2} \times 100 = 5$-th percentile (left) or $(1 - \frac{\alpha}{2}) \times 100 = 95$-th percentile (right) to signify whether the bounds inside the chance constraints are being respected. In this case, they are just outside of their bounds, which can be attributed to the fact that the voltage magnitudes were simulated using nonlinear power flow equations whereas their linearized versions were used when calculating the control bounds.

VI. Conclusion

In this paper, we proposed a novel control framework to manage the outputs of a networked stochastic system. The operational bounds on the system-wide outputs are translated into independent control bounds on each subsystem so that each subsystem can operate independently. As long as each subsystem keeps their controllable inputs within their control bounds, the system-wide outputs are guaranteed to be within their prescribed bounds with at least a specified probability. The general framework was demonstrated by applying it to the control of DERs in a distribution network to keep the voltage magnitudes within the specified bounds. It was further illustrated with numerical simulations of control

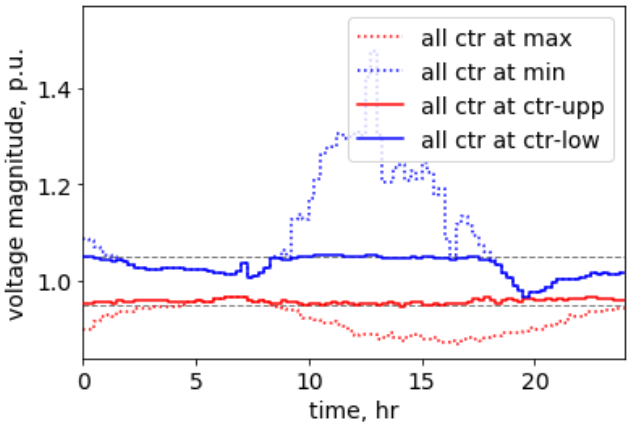

(a) Single day voltage profile

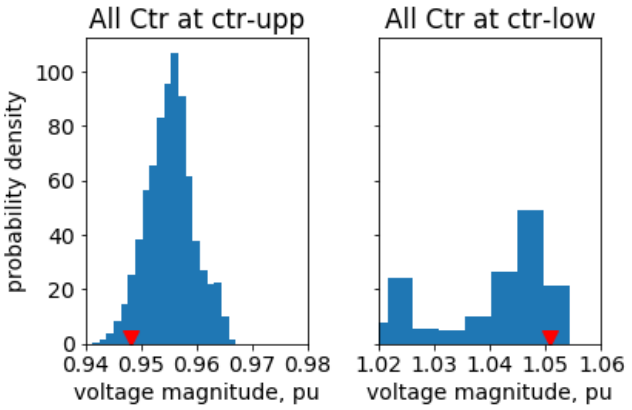

(b) Histogram of voltages

Fig. 3: (a) Voltage magnitudes vs. time, (b) histogram of voltage magnitudes at Bus 26 during the extreme cases when all controls are at their upper or lower control bounds compared to being at their maximum and minimum feasible bounds. In (b), the red triangle points to the percentiles associated with the chance constraints (9).

bounds using real-world data on an IEEE 33-bus distribution network, and it confirms the efficacy on managing voltage magnitudes. An important future direction would be to formalize how to calculate the control bounds in a distributed manner that would not require a centralized system operator.

Acknowledgment

We would like to acknowledge the work and effort put into processing the raw data to generate the feasible control bounds of each home and the forecasts of their aggregation by the research team at the Eaton Corporation, which includes Azrin Mohd Zulkefli, Arun Sukumaran Nair, Souvik Chandra, and Yi Yang.

References

[1] S. H. Chen, J. Wu, and Y. D. Chen, "Interval optimization for uncertain structures," *Finite elements in Analysis and Design*, vol. 40, no. 11, pp. 1379–1398, 2004.

[2] G. H. Huang, B. W. Baetz, and G. G. Patry, "Grey integer programming: an application to waste management planning under uncertainty," *European Journal of Operational Research*, vol. 83, no. 3, pp. 594–620, 1995.

[3] R. Liang, "Application of grey linear programming to short-term hydro scheduling," *Electric Power Systems Research*, vol. 41, no. 3, pp. 159–165, 1997.

[4] C. Huang, D. Yue, J. Xie, Y. Li, and K. Wang, "Economic dispatch of power systems with virtual power plant based interval optimization method," *CSEE journal of power and energy systems*, vol. 2, no. 1, pp. 74–80, 2016.

[5] W. Y. Tian, W. T. Sun, B. Y. Ni, J. W. Li, and Z. T. Wu, "An interval robust design optimization method and its application in heat transfer problems," *Engineering Optimization*, vol. 53, no. 10, pp. 1805–1818, 2021.

[6] D. Cai, E. Mallada, and A. Wierman, "Distributed optimization decomposition for joint economic dispatch and frequency regulation," *IEEE Transactions on Power Systems*, vol. 32, no. 6, pp. 4370–4385, 2017.

[7] G. Goel, N. Chen, and A. Wierman, "Thinking fast and slow: Optimization decomposition across timescales," in *2017 IEEE 56th Annual Conference on Decision and Control (CDC)*, pp. 1291–1298, IEEE, 2017.

[8] V. C. Gungor, D. Sahin, T. Kocak, S. Ergut, C. Buccella, C. Cecati, and G. P. Hancke, "A survey on smart grid potential applications and communication requirements," *IEEE Transactions on industrial informatics*, vol. 9, no. 1, pp. 28–42, 2012.

[9] D. Henry and J. E. Ramirez-Marquez, "Generic metrics and quantitative approaches for system resilience as a function of time," *Reliability Engineering & System Safety*, vol. 99, pp. 114–122, 2012.

[10] K. Baker, A. Bernstein, E. Dall'Anese, and C. Zhao, "Network-cognizant voltage droop control for distribution grids," *IEEE Transactions on Power Systems*, vol. 33, no. 2, pp. 2098–2108, 2017.

[11] A. Bernstein and E. Dall'Anese, "Linear power-flow models in multiphase distribution networks," in *2017 IEEE PES Innovative Smart Grid Technologies Conference Europe (ISGT-Europe)*, pp. 1–6, IEEE, 2017.

[12] K. Christakou, M. Paolone, and A. Abur, "Voltage control in active distribution networks under uncertainty in the system model: A robust optimization approach," *IEEE Transactions on Smart Grid*, vol. 9, no. 6, pp. 5631–5642, 2017.

[13] X. Chen, E. Dall'Anese, C. Zhao, and N. Li, "Aggregate power flexibility in unbalanced distribution systems," *IEEE Transactions on Smart Grid*, vol. 11, no. 1, pp. 258–269, 2019.

[14] B. Cui, A. Zamzam, and A. Bernstein, "Network-cognizant time-coupled aggregate flexibility of distribution systems under uncertainties," in *2021 American Control Conference (ACC)*, pp. 4178–4183, IEEE, 2021.

[15] "Pecan Street Dataport," Sep 2021. Pecan Street Inc. [Online]. Available: `https://www.pecanstreet.org/dataport/`.

[16] M. E. Baran and F. F. Wu, "Network reconfiguration in distribution systems for loss reduction adn load balancing," *IEEE transactions on power delivery*, vol. 4, no. 2, pp. 1401–1407, 1989.

[17] L. Thurner, A. Scheidler, F. Schäfer, J. Menke, J. Dollichon, F. Meier, S. Meinecke, and M. Braun, "Pandapower—an open-source python tool for convenient modeling, analysis, and optimization of electric power systems," *IEEE Transactions on Power Systems*, vol. 33, no. 6, pp. 6510–6521, 2018.

[18] G. C. Calafiore and L. El Ghaoui, "On distributionally robust chance-constrained linear programs," *Journal of Optimization Theory and Applications*, vol. 130, no. 1, pp. 1–22, 2006.

[19] J. Comden, A. S. Zamzam, and A. Bernstein, "Data-driven moment-based distributionally robust chance-constrained optimization," *arXiv preprint arXiv:2109.08742*, 2021.